Graphene Oxide

DOI: 10.1002/ange.201309931

Proton Conductivities of Graphene Oxide Nanosheets: Single, Multilayer, and Modified Nanosheets

Kazuto Hatakeyama, Mohammad Razaul Karim, Chikako Ogata, Hikaru Tateishi, Asami Funatsu, Takaaki Taniguchi, Michio Koinuma, Shinya Hayami, and Yasumichi Matsumoto**

Abstract: *Proton conductivities of layered solid electrolytes can be improved by minimizing strain along the conduction path. It is shown that the conductivities (σ) of multilayer graphene oxide (GO) films (assembled by the drop-cast method) are larger than those of single-layer GO (prepared by either the drop-cast or the Langmuir-Blodgett (LB) method). At 60 % relative humidity (RH), the σ value increases from 1×10^{-6} S cm^{-1} in single-layer GO to 1×10^{-4} and 4×10^{-4} S cm^{-1} for 60 and 200 nm thick multilayer films, respectively. A sudden decrease in conductivity was observed for with ethylenediamine (EDA) modified GO (enGO), which is due to the blocking of epoxy groups. This experiment confirmed that the epoxide groups are the major contributor to the efficient proton transport. Because of a gradual improvement of the conduction path and an increase in the water content, σ values increase with the thickness of the multilayer films. The reported methods might be applicable to the optimization of the proton conductivity in other layered solid electrolytes.*

The worldwide research on ion conductivity aims at designing cheap, stable, inert, and solid superionic conductors for fuel-cell applications.[1] Usually, a polymeric support with hydrophilic sites, which facilitate the adsorption of moisture and the propagation of protons through the attached water film, is used for designing superionic conductors. Graphene oxide (GO) possesses all of these essential properties and has been shown to be a promising candidate for such applications.[2] The proton conductivities of GO and of some related hybrids and derivatives have been reported only in recent years.[3] In all of these reports, the conductivity measurements were performed on pellet samples, where the GO nanosheet could be oriented in both a parallel and a perpendicular direction with respect to the electrode assembly. These different arrangements restrict the conductivity, as protons moving over a horizontally lying GO nanosheet might suffer from some restraints when they try to penetrate the benzene-like carbon sieve of perpendicularly positioned GO fragments. The improved conductivity in polymeric materials that have a one-dimensional pathway supports this hypothesis.[4] We have previously shown that the in-plane conductivity of a GO nanosheet was higher than that of a pellet sample.[5] We predicted that the conduction pathway through intercalated GO channels should be faster than on the GO surface because of the support of two GO walls and improved hydration dynamics. Herein, we report the design of bundles of horizontal, GO walled channels in a multilayer assembly. The conductivity increased significantly, and the σ value was found to be proportional to the thickness of the multilayer GO film.

As GO bears various hydrophilic functional groups, it is necessary to identify the main factors that influence proton conductivity in GO for further advancements in this field. We previously observed strong electrostatic attractions between the negatively charged epoxy groups of GO and transition-metal ions.[6] Based on this observation, we herein describe how the epoxy sites could be successfully blocked with ethylenediamine to yield enGO. The decrease in conductivity that was observed with enGO confirmed that the epoxy sites act as the major vehicle for proton transport in GO.

Two different single-layer GO samples were fabricated on comb electrodes (Supporting Information, Figure S1) using either the Langmuir–Blodgett (LB) assembly method or the drop-cast method (Figures S2, S3). The single- and multilayer natures of the GO films were confirmed by atomic force microscopy (AFM) and scanning electron microscopy (SEM; Figure 1; see also Figure S4). The σ values were calculated using the formula $\sigma = L/(R\times T\times D)$, where R, L, T, and D are the measured resistance (Figure S5), width, thickness, and length of the samples (see the Supporting Information).

The σ value for single-layer GO increased almost linearly from 6×10^{-7} S cm^{-1} at 55 % relative humidity (RH) to 2×10^{-4} S cm^{-1} at 90 % RH (Figure 2a). Other samples behaved similarly. The conductivities also increased with film thickness. At 60 % RH, the σ value increased from 1×10^{-6} S cm^{-1} in single-layer GO to 1×10^{-4} and 4×10^{-4} S cm^{-1} for films with a thickness of 60 and 200 nm, respectively. Accordingly, the σ value (2×10^{-3} S cm^{-1}) that we previously reported for a 18 μm thick GO paper complies with the present observation.[7] The conductivity of a 160 nm thick enGO film exhibited a sudden fall. Although an enGO film is generally much thicker, its typical conductivity value (7×10^{-6} S cm^{-1} at 60 % RH) is lower than that of the 60 nm thick multilayer GO film by one order of magnitude. The RH dependencies of the conductivities of various GO films are different. The diver-

[*] K. Hatakeyama, M. R. Karim, C. Ogata, H. Tateishi, Dr. A. Funatsu, Prof. T. Taniguchi, Prof. M. Koinuma, Prof. S. Hayami, Prof. Y. Matsumoto
Graduate School of Science and Technology, Kumamoto University
2-39-1 Kurokami, Chuo-ku, Kumamoto 860-8555 (Japan)
and
JST, CREST, Gobancho
7 Gobancho, Chiyoda-ku, Tokyo, 102-0076 (Japan)
E-mail: hayami@sci.kumamoto-u.ac.jp
yasumi@gpo.kumamoto-u.ac.jp

Supporting information for this article is available on the WWW under http://dx.doi.org/10.1002/anie.201309931.

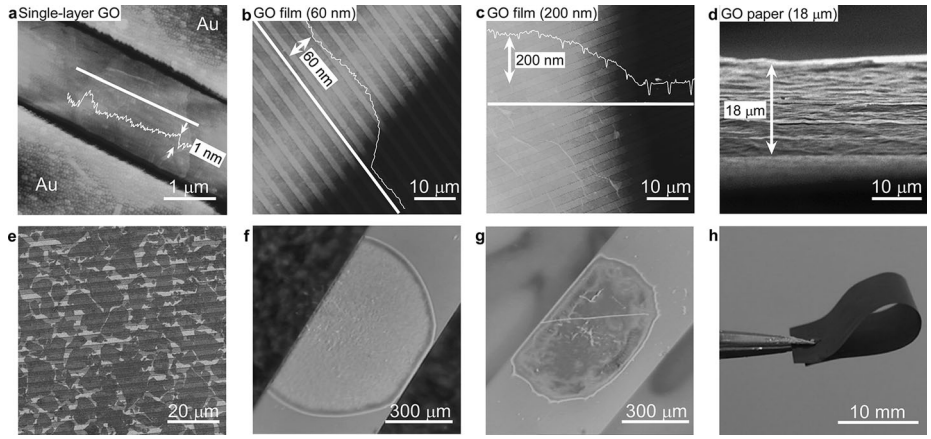

Figure 1. GO samples on comb electrode pairs. AFM images of a) single-layer GO (LB film) and of b) 60 and c) 200 nm thick multilayer GO (drop-cast films). SEM images of d) 18 μm thick GO paper[7] and e) single-layer GO (LB film). Charge-coupled device (CCD) images of f) 60 nm and g) 200 nm thick GO films on a comb electrode. h) Photograph of GO paper.

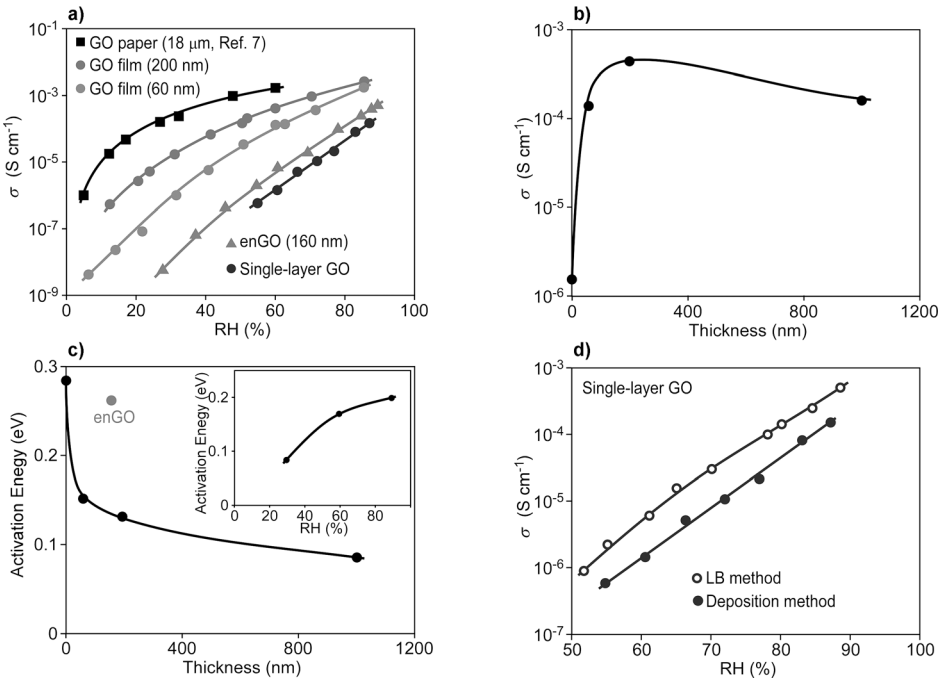

Figure 2. a) Dependence of the proton conductivities of various GO films on RH at 25 °C (thicknesses of the GO films are given in parentheses). b) Dependence of the conductivities on the thickness of the material. c) Dependence of the E_a values on the thickness of the GO films at 60% RH. Inset: Dependence of the E_a values of the GO film (thickness: 150 nm) on RH. d) RH-dependent conductivities of single-layer GO produced by either the LB or the drop-cast method.

gence and convergence of the lines at low (< 40%) and high RH, respectively indicate that the thickness dependence of the σ values is more pronounced at a low water content. The σ value increases steeply up to a thickness of 200 nm, beyond which a saturated state with a σ value of approximately 4×10^{-4} S cm^{-1} is attained (Figure 2b). The temperature-dependent conductivities and Arrhenius plots with activation energies (E_a) are shown in Figures S6 and S7. The E_a value is at its highest (0.28 eV) for single-layer GO and decreases sharply with film thickness up to 200 nm, beyond which a stable value of approximately 0.08 eV is reached (Figure 2c). The E_a value of the enGO film is 0.26 eV, which is almost twice the value of the GO film with a similar thickness. The incremental increase in the E_a value with RH is consistent with previous reports (Figure 2c, inset).[8] The E_a value for the 150 nm thick GO film increased from 0.08 eV at 30% RH to 0.2 eV at 90% RH. The σ value for a single-layer LB GO film is approximately five times larger than that for the drop-cast film (Figure 2d).

The in-plane and through-plane conductivities of a proton conductor are not necessarily the same.[9] According to Meyer's hypothesis, a very thin film (less than four times the Debye length) should exhibit very high in-plane ionic conductivity.[10] Therefore, the high conductivity of the nanometer-sized GO sheet matches our expectations. The thickness dependence of the in-plane σ values is supposed to be governed by the water content and the hydration behavior of the GO material. The hydration properties and water dynamics of oxidized graphitic materials have previously been studied by several groups.[8,11] The hydrophilic functional groups (OH, COOH, and C–O–C) in a GO nanosheet[12] adsorb water and support both the upstream and downstream fluxes of protons, which results in higher conductivity. The multilayer film adopts the shape of a compact bundle of numerous two-dimensional conductive channels. Compared with single-layer GO, both the water content and the hydration dynamics are improved in such bundles in several ways. First, the interlayer space contains an increased amount of hydrophilic groups that extend from the two GO walls and support a higher water content. This higher amount of water results in a larger and more flexible interlayer distance.[13] We propose that this larger and more flexible cavity speeds up proton movement and hydrogen bond reformation processes. Second, the rate of hydrogen bond reformation is also accelerated in the presence of two opposite GO walls (Figure 3a). Finally, we suggest that in a multilayer assembly, the propagating protons have the

option to change the conduction path (Figure 3a). The mobilized protons in GO can change their path from one layer to one of the surrounding layers through numerous nanopores.[14] These alternative conduction pathways support faster ion movement. The divergence of the lines for different GO films at low RH is significant (Figure 2a). By thermogravimetric analysis (TGA), we determined the water content in the 18 μm thick GO paper at 30 and 90% RH to be approximately 21 and 31 wt%, respectively (Figure S8). It seems that at high RH, the water content increases only to a limited extent, which might cause the observed convergence effect. Furthermore, an excess amount of water molecules in the interlayer space might also play a role. Although an increased amount of water provides a faster pathway for proton propagation, excess water results in some suppression of the proton movement, which is negligible at low RH. This fact is also supported by the increase in the E_a values with respect to RH (inset of Figure 2c). The decrease in the E_a values with increasing film thickness complies with an increase in the σ values for thicker films (Figure 2c).

The adsorbed water molecules can generate protons through the self-dissociation process reported by Kreuer.[15] The decrease in conductivity that results from the blocking of some epoxy groups in enGO confirmed that the epoxide groups are the major contributor to efficient proton transport (Figure 2a). The amount of C–O–C, C=O, and O=C–O groups in enGO is reduced by 82.89, 5.77, and 56.75%, respectively (Figure S9). Therefore, the decrease in conductivity is principally associated with a reduction in the number of epoxy groups. The O=C–O moieties do not play a role in proton conduction as in photoreduced GO, the conductivity decreased even when the relative amount of O=C–O moieties increased (Figure S10). The O=C–O and C=O groups are located at the edge of the GO nanosheet, whereas the C–O–C moieties are located only in the interior of the GO nanosheet.[16] Therefore, the major in-plane journey of protons in the interior of a nanosheet is supported only by the epoxy groups. The high E_a value of enGO corroborates the impaired proton conductivity (Figure 2c). The higher conductivity in LB single-layer GO results from a continuous and wider pathway that is obtained by the joining of small GO fragments (Figure 2d). The low E_a values (< 0.3 eV) for all of the samples imply that a Grotthuss mechanism is operating,[17] which is commonly the case for proton conductivity through a H_2SO_4 solution[18] and in Nafion.[19] A proposed mechanism for proton conductivity in GO is shown in Figure 3. In multilayer GO, mobilized protons can change path from one layer to the surrounding layers through nanopores, which results in increased conductivity. Proton mobility and hydrogen bond reformation in single- and multilayer GO films is supported by single and double GO walls, respectively.

In conclusion, because of a gradual improvement in conduction pathway, hydration dynamics, and water content, the in-plane proton conductivities of various GO samples follows the following trend: pellet GO[5] < single-layer GO (drop-cast film < LB film) < multilayer GO (thin film < thick film < GO paper[7]). The proton conductivities of multilayer GO films are thickness-dependent and higher than that of single-layer GO by several orders of magnitude. The ion conductivity is mainly supported by epoxy groups, which was revealed by the lower conductivities of enGO, which lacks epoxy groups, and photoreduced GO. The low E_a values indicate that these GO materials might be suitable for practical applications.

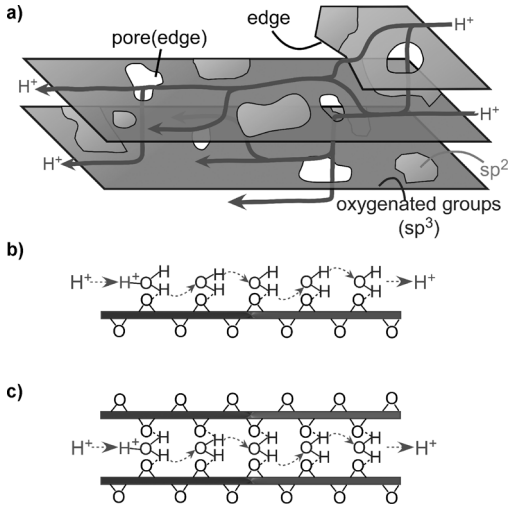

Figure 3. Proposed mechanism for proton conductivity. a) In multilayer GO, protons can change from the conduction path in one layer to another through nanopores. The sp^3- and sp^2-hybridized areas are denoted in dark gray and light gray, respectively. Proton transfer supported by single (b) and double (c) GO walls, respectively.

Received: November 15, 2013
Revised: March 26, 2014
Published online: May 18, 2014

Keywords: electrochemistry · epoxy groups · graphene oxide · layered compounds · proton conductivity

[1] a) G. A. Voth, *Acc. Chem. Res.* **2006**, *39*, 143–150; b) T. Kudo, K. Fueki, *Solid State Ionics*, 1st ed., VCH, Weinheim, **1990**.
[2] a) M. Acik, C. Mattevi, C. Gong, G. Lee, K. Cho, M. Chhowalla, Y. J. Chabal, *ACS Nano* **2010**, *4*, 5861–5868; b) Y. W. Zhu, S. Murali, W. W. Cai, X. S. Li, J. W. Suk, J. R. Potts, R. S. Ruoff, *Adv. Mater.* **2010**, *22*, 3906–3924.
[3] a) J. H. Jung, J. H. Jeon, V. Sridhar, I. K. Oh, *Carbon* **2011**, *49*, 1279–1289; b) H. Zarrin, D. Higgins, Y. Jun, Z. W. Chen, M. Fowler, *J. Phys. Chem. C* **2011**, *115*, 20774–20781; c) K. Raidongia, J. Huang, *J. Am. Chem. Soc.* **2012**, *134*, 16528–16531; d) Ravikumar, K. Scott, *Chem. Commun.* **2012**, *48*, 5584–5586.
[4] T. Yamada, M. Sadakiyo, H. Kitagawa, *J. Am. Chem. Soc.* **2009**, *131*, 3144–3145.
[5] M. R. Karim, K. Hatakeyama, T. Matsui, H. Takehira, T. Taniguchi, M. Koinuma, Y. Matsumoto, T. Akutagawa, T. Nakamura, S. Noro, T. Yamada, H. Kitagawa, S. Hayami, *J. Am. Chem. Soc.* **2013**, *135*, 8097–8100.
[6] M. R. Karim, H. Shinoda, M. Nakai, K. Hatakeyama, H. Kamihata, T. Matsui, T. Taniguchi, M. Koinuma, K. Kuroiwa, M. Kurmoo, Y. Matsumoto, S. Hayami, *Adv. Funct. Mater.* **2013**, *23*, 323–332.
[7] H. Tateishi, K. Hatakeyama, C. Ogata, K. Gezuhara, J. Kuroda, A. Funatsu, M. Koinuma, T. Taniguchi, S. Hayami, Y. Matsumoto, *J. Electrochem. Soc.* **2013**, *160*, F1175–F1178.

[8] A. Buchsteiner, A. Lerf, J. Pieper, *J. Phys. Chem. B* **2006**, *110*, 22328 – 22338.
[9] T. Y. Soboleva, Z. Xie, Z. Q. Shi, E. Tsang, T. C. Navessin, S. Holdcroft, *J. Electroanal. Chem.* **2008**, *622*, 145 – 152.
[10] a) J. Maier, *Solid State Ionics* **1987**, *23*, 59 – 67; b) J. Maier, *Solid State Ionics* **2003**, *157*, 327 – 334.
[11] a) S. Cerveny, F. Barroso-Bujans, A. Alegria, J. Colmenero, *J. Phys. Chem. C* **2010**, *114*, 2604 – 2612; b) A. Lerf, A. Buchsteiner, J. Pieper, S. Schottl, I. Dekany, T. Szabo, H. P. Boehm, *J. Phys. Chem. Solids* **2006**, *67*, 1106 – 1110.
[12] a) J. A. Yan, L. D. Xian, M. Y. Chou, *Phys. Rev. Lett.* **2009**, *103*, 086802 – 086805; b) A. Lerf, H. Y. He, M. Forster, J. Klinowski, *J. Phys. Chem. B* **1998**, *102*, 4477 – 4482.
[13] V. M. Gun'ko, V. V. Turov, R. L. D. Whitby, G. P. Prykhod'ko, A. V. Turov, S. V. Mikhalovsky, *Carbon* **2013**, *57*, 191 – 201.
[14] K. Erickson, R. Erni, Z. Lee, N. Alem, W. Gannett, A. Zett, *Adv. Mater.* **2010**, *22*, 4467 – 4472.
[15] K. D. Kreuer, *Chem. Mater.* **1996**, *8*, 610 – 641.
[16] D. R. Dreyer, S. Park, C. W. Bielawski, R. S. Ruoff, *Chem. Soc. Rev.* **2010**, *39*, 228 – 240.
[17] N. Agmon, *Chem. Phys. Lett.* **1995**, *244*, 456 – 462.
[18] Y. K. Choe, E. Tsuchida, T. Ikeshoji, *J. Chem. Phys.* **2007**, *126*, 154510.
[19] a) K. A. Mauritz, R. B. Moore, *Chem. Rev.* **2004**, *104*, 4535 – 4585; b) Y. K. Choe, E. Tsuchida, T. Ikeshoji, S. Yamakawa, S. Hyodo, *Phys. Chem. Chem. Phys.* **2009**, *11*, 3892 – 3899.